International Journal of Heat and Mass Transfer 52 (2009) 2704–2713

Contents lists available at ScienceDirect

International Journal of Heat and Mass Transfer

journal homepage: www.elsevier.com/locate/ijhmt

Heat and mass transfer in plate-fin enthalpy exchangers with different plate and fin materials

Li-Zhi Zhang *

Key Laboratory of Enhanced Heat Transfer and Energy, Conservation of Education Ministry, School of Chemistry and Chemical Engineering, South China University of Technology, Guangzhou 510640, China

ARTICLE INFO

Article history:
Received 15 May 2008
Received in revised form 5 December 2008
Available online 21 February 2009

Keywords:
Heat transfer
Mass transfer
Energy recovery
Supported liquid Membranes
Plate-fin

ABSTRACT

Enthalpy exchangers have been used as an efficient means to recover both sensible heat and moisture from exhaust ventilation air. A cross-flow plate-fin structure is the most popular arrangement for the exchanger core due to its compactness and high mechanical strength even with very small channel wall thickness. Traditionally, hygroscopic paper is selected as the plate and fin materials. Though the sensible effectiveness with this material is satisfactorily high, the latent effectiveness is disappointingly low due to the low moisture diffusivity in paper. To solve this problem, in this study, a novel concept is proposed to augment moisture transfer in the exchanger. Plates and fins are made with different materials. A novel membrane – the composite supported liquid membrane (CSLM) is used as the plate material. Paper is still used as the fin material for its cheapness and high support strength. To make comparisons, two cores, one is paper-fin and paper-plate, and another one is paper-fin and membrane-plate, are constructed and tested for heat and moisture recovery. Simultaneous heat and moisture transfer in the plate-fin core is studied. Mathematical model governing the heat and moisture transfer in the cores is set up and numerically solved. Both the experimental data and numerical results indicate that the latent effectiveness of the paper-fin and membrane-plate core is 60% higher than the traditional paper-fin and paper-plate core, due to the high moisture diffusivity in the CSLM.

1. Introduction

Air-conditioning in hot and humid environments is an essential requirement for support of daily human activities. Humidity problems can be found in many applications including office buildings, supermarkets, art galleries, museums, libraries, electronics manufacturing facilities, pharmaceutical clean rooms, indoor swimming pools and other commercial facilities. For thermal comfort reasons, indoor air conditions around 25 °C temperature and 10 g/kg humidity ratio are the accepted set points. However, the Southern China and other Southeast Asia countries have a long summer season with a daily average temperature of 30 °C, and humidity ratio above 20 g/kg. Outdoor relative humidity often exceeds 80% continuously for a dozen of days, leading to mildew growth on wall and furniture surfaces, which affects people's life seriously. In spring in Southern China, there is a period named "Plum raining seasons" when it rains continuously for one to two months. People can not see sun for a long time and stuff from quilts to grains gets moldy easily. Consequently, mechanical air dehumidification plays a major role in air conditioning industry in these regions. In many of these countries, the energy used to cool and dehumidify the ventilation air ranges from 20% to 40% of the total energy consumption for air conditioning, and can be even higher where 100% fresh air ventilation is required [1], such as kitchen, hospital, factories.

Enthalpy exchangers (or the so-called energy recovery ventilators) [2,3] could save a large fraction of the energy for cooling and dehumidification since cool and dryness would be recovered from the exhaust stream to the fresh air in summer. With enthalpy exchangers, the efficiency of existing HVAC systems can also be improved. The reason is that normally the fresh air is dehumidified by cooling coil through condensation followed by a re-heating process, which is very energy intensive. Besides energy conservation, the enthalpy exchangers have the additional benefits of ensuring sufficient fresh air supply, which is crucial for the prevention of epidemic respiratory diseases like SARS and Bird flu.

As other air-to-air heat exchangers, sinusoidal plate-fin channels are the popular structure for enthalpy exchanger cores. The structure, as depicted in Fig. 1 for the whole core and Fig. 2 for a single duct geometry, respectively, is preferred because it has many virtues like it is stationary, compact, and easy to construct. The differences between enthalpy exchangers and other air-to-air heat exchangers are that in place of metal materials, current commercial enthalpy exchangers employ hygroscopic paper as the

* Tel./fax: +86 20 87114268.
E-mail address: Lzzhang@scut.edu.cn

0017-9310/$ - see front matter © 2009 Elsevier Ltd. All rights reserved.
doi:10.1016/j.ijheatmasstransfer.2008.12.014

Nomenclature

A	Area (m^2)
c_p	specific heat (kJ kg^{-1} K^{-1})
D	diffusivity (m^2/s)
D_h	hydrodynamic diameter (m)
dP	pressure drop (Pa)
f_c	channel friction coefficient
f_L	local friction coefficient
G	mass flow rate (kg/s)
h	convective heat transfer coefficient (kW m^{-2} K^{-1})
E	emission rate (kg m^{-2} s^{-1})
k	convective mass transfer coefficient (m/s)
k_p	partition coefficient
NTU	number of transfer units
Nu	Nusselt number
n	number of channels for each flow
RH	relative humidity
Sh	Sherwood number
T	temperature (K)
u_a	air bulk velocity (m/s)
v	hydrodynamic viscosity (m^2/s)
x	coordinate (m)
x_F	channel length (m)
y_F	channel length (m)
y	coordinate (m)

Greek letters

ρ	density (kg/m^3)
λ	heat conductivity (W m^{-1} K^{-1})
ω	humidity ratio (kg moisture/kg air)
ε	effectiveness
ϕ	porosity
δ	thickness (μm)
Ω	fin conductance parameter

Superscripts

*	dimensionless

Subscripts

a	air
e	exhaust air
f	fresh air
fin	fins
i	inlet
L	latent
mem	membrane
o	outlet
pla	plates
s	sensible

material for fins and plates, to transfer both sensible heat and moisture simultaneously.

Moisture diffusivity in solid materials including paper is quite low, in the order of 10^{-12}–10^{-13} m^2/s [4,5]. As a result, the latent effectiveness of current enthalpy exchangers is quite limited due to such small moisture transfer rates. In fact, the low latent effectiveness of current enthalpy exchangers has impeded its market penetrations. In contrast, moisture diffusion in liquids ($\sim 10^{-9}$ m^2/s [6,7]) is several orders higher than that in solids. For this reason, in recent years, a novel material, the composite supported liquid membrane (CSLM), which used a liquid membrane to selectively transfer moisture, has been proposed [8]. According to this concept, a layer of liquid LiCl solution was immobilized in a porous solid support membrane to transfer moisture while impeding other unwanted gases like CO_2. To protect the liquid membrane inside, two porous hydrophobic PVDF (Polyvinylidene Fluoride) layers were formed on both surfaces of the supported liquid membrane. The final micro-structure is shown in Fig. 3. As seen, there are totally three layers: two PVDF porous skin layers and a porous AC (Acetate Cellulose) layer which is to support the liquid LiCl solution in its macro and micro pores. With this novel membrane, the latent effectiveness is expected to be improved substantially.

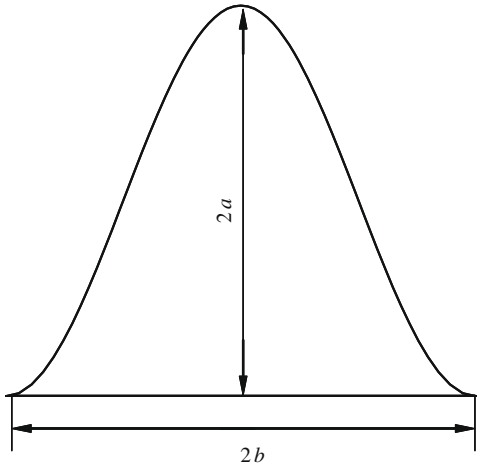

Fig. 2. Geometries of a sinusoidal plate-fin duct.

Much effort has been focused on the fabrication of CSLM [8] and the measurements of heat and moisture transfer properties through a single CSLM layer [9]. However, studies of heat mass

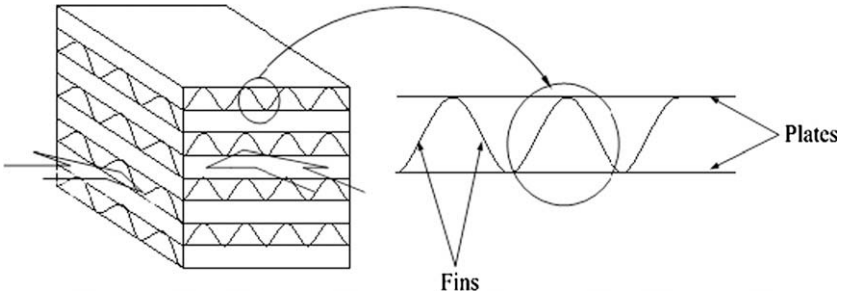

Fig. 1. Schematic of a cross-flow plate-fin heat exchanger with sinusoidal passages.

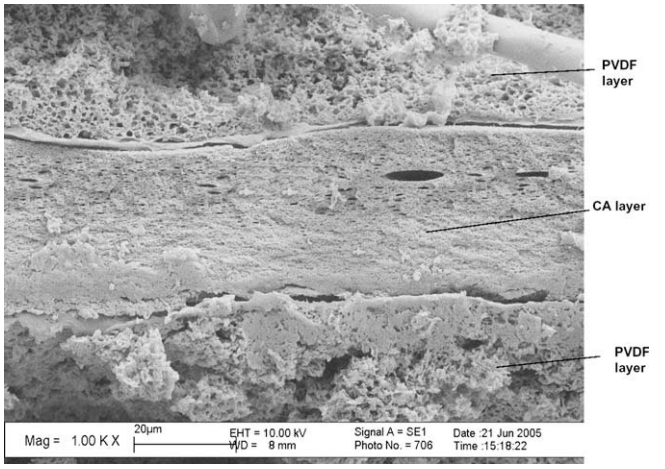

Fig. 3. Scanning Electron Microscope (SEM) graph of the composite supported liquid membrane (CSLM).

transfer through CSLM in an enthalpy exchanger, especially in the form of plate-fin structure, has not been found. This problem will be addressed in this paper. The study is a step forward toward its real applications in enthalpy exchangers. The idea is to build a commercial scale plate-fin exchanger core with the fabricated CSLMs. Rather than using hygroscopic paper as the material for the whole core, the new core uses the novel CSLM as the plate material. Paper is still used as the fin material because it is more rigid and cheaper than membranes. Necessary mechanical strength is required for selecting fin materials and paper is proved to be a good fin material. Moisture transfer is intensified by the use of CSLM as plates. To make comparisons, a common core with paper-plates and paper-fins are also built. Both experimental and numerical investigations are conducted to compare the performances with these two types of cores. Further, the coupled heat and moisture transfer in the plate-fin exchanger is studied. A literature review found that heat and mass transfer in a single plate-fin duct with finite fin conductance have been studied [10], however heat and mass transfer in a whole exchanger which is comprised of numerous plate-fin channels have not been mentioned.

2. Experimental work

The purpose of the experiment is to measure the steady state heat and moisture transfer through the enthalpy exchanger cores, by the measurements of inlet and outlet temperature, humidity and air flow rates. The sensible and latent effectiveness and pressure drop are the performance indices.

2.1. Test-rig

A schematic of the test-rig is shown in Fig. 4. Fig. 4(a) shows the ducting work and Fig. 4(b) shows the core structure. Two parallel air ducts with a 200 × 200 mm cross section are assembled. Each duct is comprised of a variable speed blower, a wind tunnel, a set of nozzles, wind straightenners, electric heating coils, steam humidification tubes, temperature and humidity sensors. An exchanger shell is designed to hold the core. The small converging wind tunnels produce steady, homogeneous, fully developed air flow to the exchanger. The heating power and the steam generation currents can be adjusted according to the set points temperature and humidity. After the air temperature and humidity are adjusted to the set points, the two ducts are connected to the two inlets of the exchanger shell, respectively. The exchanger shell is designed to station the exchanger core and separate the cross-flow two air streams. The cores, either all-paper or paper-fin and membrane-plate, can be inserted into the quadrate cavity in the center of the shell. The whole test rig is built in a constant temperature and constant humidity room, so the inlet temperature and humidity can be controlled and maintained very well even under very hot and humid ambient weather conditions. A 10 mm thick plastic foam insulation layer is pasted on the outer surfaces of the ducts and the shells to prevent heat dissipation from the system to the surroundings. Moisture dissipation from air stream to the surroundings is negligible since the duct and shell materials are highly hydrophobic and they could adsorb little moisture. The heat loss from the system is below 0.5%, and moisture loss is less than 0.1%.

The nominal operating conditions: fresh air inlet 35 °C and 0.021 kg/kg; exhaust air inlet 27 °C and 0.012 kg/kg. The corresponding inlet relative humidity (*RH*) is 59% and 54% for fresh air and exhaust air, respectively. During the experiment, equal air flow rates are kept for the two ducts. The design air flow rates are 150 m^3/h. In the test, they are changed by variable speed blowers, to have different air velocities. Humidity, temperature, and volumetric flow rates are monitored at the inlet and outlet of the exchanger. Before and after each test, temperature and humidity sensors are calibrated with a Pt-100 temperature sensor and a chilled-mirror dew-point meter. Hot-wire anemometers that are used to measure the wind speed before and after the exchanger are compared with the air flow rates measured by nozzles. The offset is controlled to within 1% limit. Volumetric air flow rates are varied from 100 m^3/h to 200 m^3/h, corresponding to frontal air velocities from 0.37 m/s to 0.74 m/s which are typical for commercial enthalpy exchangers. Air flow under such conditions is laminar, with Reynolds numbers not exceeding 200. A digital pressure differential gauge is used to measure the pressure drop across the tested core. The uncertainties are: temperature ±0.1 °C; humidity ±2%; volumetric flow rate ±1%, pressure drop ±1%. The final uncertainty is ±4.5% for sensible and latent effectiveness. Six sensors are uniformly positioned on the inlet and outlet surfaces of the shell to have a mean value of measurements. Due to the small channels in the core, outlet air from the core is quite evenly distributed. In other words, the core itself has the effect of another ideal wind straightener. Anyway, another six wind straighteners, which are made of plates with numerous evenly distributed small holes drilled, are installed in the ducts before and after the shell and nozzles to well distribute the wind. In addition, heat and mass balance between the fresh air and the exhaust air are checked. Their differences are controlled to be less than 0.1%. From these preparatory works, the test rig is considered to be reliable.

After the measurement of mean inlet and outlet temperature and humidity, the sensible and latent effectiveness are calculated by

$$\varepsilon_s = \frac{T_{fi} - T_{fo}}{T_{fi} - T_{ei}} \quad (1)$$

$$\varepsilon_L = \frac{\omega_{fi} - \omega_{fo}}{\omega_{fi} - \omega_{ei}} \quad (2)$$

where T and ω are temperature (°C) and humidity ratio (kg moisture/kg dry air), respectively. Subscripts "f", "e", "i", "o" refer to fresh air, exhaust air, inlet and outlet, respectively. The sensible effectiveness and the latent effectiveness are the key performance indexes to evaluate an enthalpy exchanger.

2.2. Cores

Two cores, one is paper-plate and paper-fin (core 1), another one is paper-fin and CSLM-plate (core 2), are built. They have the same structural parameters as shown in Table 1. Their dimensions are the same and they are equal to the dimensions of the cavity in-

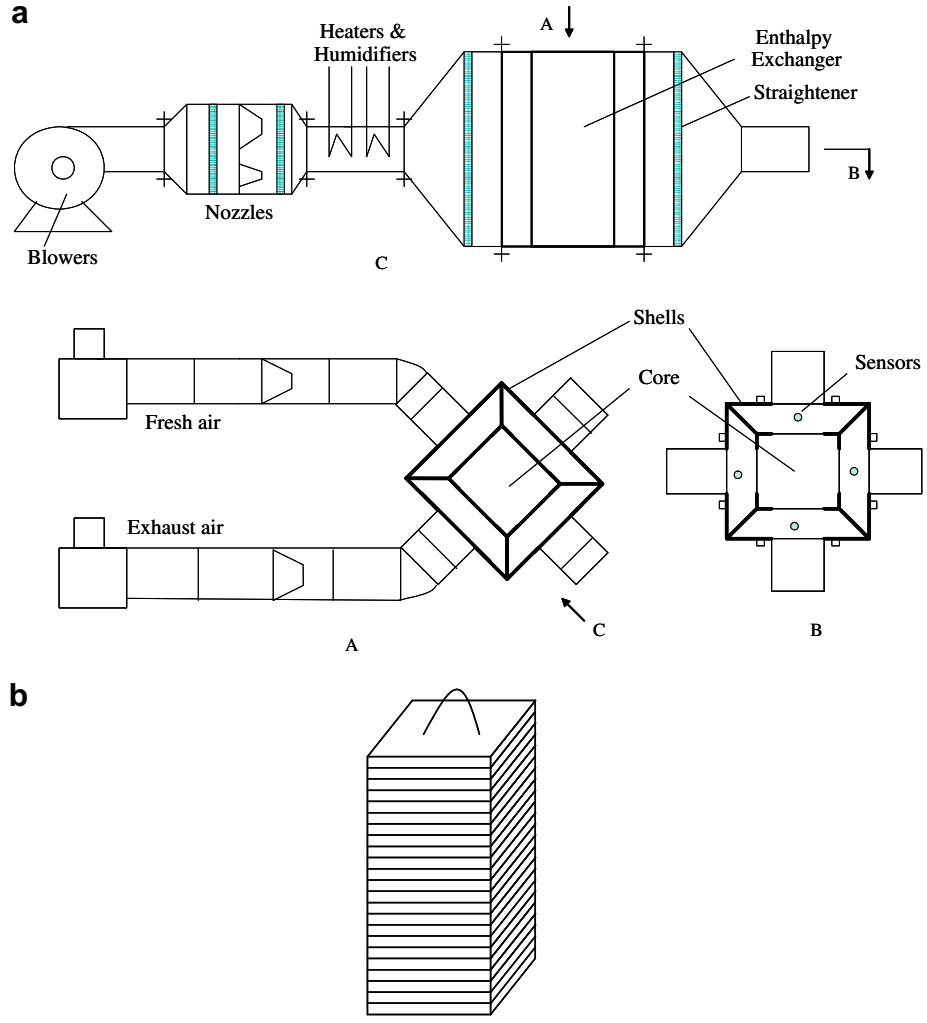

Fig. 4. Experimental set-up of the enthalpy exchanger. (a) The duct work; (b) the core.

Table 1
Structural and physical parameters of the two cores.

Symbol	Unit	Value	Symbol	Unit	Value
n		115	a	mm	1
x_F, y_F	mm	185	b	mm	2.5
δ_{fin}	μm	100	δ_{pla}	μm	90
k_P		0.58	D_{fin}	m^2/s	3.56e−11
D_{mem}	m^2/s	5.51e−10	D_a	m^2/s	2.82×10^{-5}
λ_{fin}	$W\,m^{-1}\,K^{-1}$	0.44	λ_{mem}	$W\,m^{-1}\,K^{-1}$	0.42
λ_a	$W\,m^{-1}\,K^{-1}$	0.0263	v	m^2/s	15.89e−6
ρ_a	kg/m^3	1.18	ρ_{mem}	kg/m^3	860
ρ_{fin}	kg/m^3	800	RH_{fi}		0.59
T_{fi}	°C	35	RH_{ei}		0.52
T_{ei}	°C	27			

side the shell. So they can be replaced and inserted into the shell conveniently. After the core is placed in the shell, correct sealing are undertaken to ensure air cross-over is less than 1%.

3. Mathematical model

3.1. Heat and mass transfer in air streams

A meso-scopic model is set up. Each channel cross section is represented by one temperature or humidity. The temperature and humidity vary along flow directions (x for fresh air and y for exhaust air) and the corresponding cross directions (y for fresh air and x for exhaust air) simultaneously. On each channel cross section, though temperature and humidity are two-dimensionally different locally, as studied in [10], in this study for the whole exchanger, they are represented by a lumped parameter for each channel cross section. It can be considered as a semi-lumped parameter model. The two air streams, one hot and humid (fresh air), and the other cool and dry (exhaust air), exchange both sensible heat and moisture simultaneously in the exchanger in a cross-flow arrangement. Two-dimensional heat mass transfer model can be set up to govern the energy and mass conservations in the two air streams:

$$\frac{\partial T_f^*}{\partial x^*} = NTU_{sf}(T_{mf}^* - T_f^*) \tag{3}$$

$$\frac{\partial T_e^*}{\partial y^*} = NTU_{se}(T_{me}^* - T_e^*) \tag{4}$$

$$\frac{\partial \omega_f^*}{\partial x^*} = NTU_{Lf}(\omega_{mf}^* - \omega_f^*) \tag{5}$$

$$\frac{\partial \omega_e^*}{\partial y^*} = NTU_{Le}(\omega_{me}^* - \omega_e^*) \tag{6}$$

where x is flow direction for fresh stream and y is flow direction for exhaust stream.

The dimensionless temperature and humidity are defined by

$$T^* = \frac{T - T_{ei}}{T_{fi} - T_{ei}} \tag{7}$$

$$\omega^* = \frac{\omega - \omega_{ei}}{\omega_{fi} - \omega_{ei}} \tag{8}$$

The dimensionless coordinates are defined by

$$x^* = \frac{x}{x_F} \tag{9}$$

$$y^* = \frac{y}{y_F} \tag{10}$$

where x_F and y_F are channel lengths for fresh air and exhaust air (m). Here $x_F = y_F$. The air side number of transfer units for heat and moisture are defined by

$$NTU_{sf} = \frac{(hA)_f}{(Gc_p)_f} \tag{11}$$

$$NTU_{se} = \frac{(hA)_e}{(Gc_p)_e} \tag{12}$$

$$NTU_{Lf} = \frac{(\rho_a kA)_f}{(G)_f} \tag{13}$$

$$NTU_{Le} = \frac{(\rho_a kA)_e}{(G)_e} \tag{14}$$

where k and h are air side convective mass transfer coefficient (m/s) and convective heat transfer coefficient (kW m^{-2} s^{-1}), respectively; G is air mass flow rate (kg/s); A is total transfer area including plates and fins (m^2) for each stream; c_p is specific heat (kJ kg^{-1} K^{-1}). Subscripts "f" refers to fresh side and "e" refers to exhaust side; "s" refers to sensible and "L" refers to latent; "mf" refers to membrane surface on fresh side, and "me" refers to membrane surface on exhaust side.

The outlet temperature and humidity values are calculated by Eqs. (3)–(6). Then it is convenient to calculate sensible and latent effectiveness from Eqs. (1) and (2). Humidity ratios can be converted to relative humidity from psychrometric chart.

The convective heat transfer coefficient and mass transfer coefficient can be calculated by

$$Nu = \frac{hD_h}{\lambda_a} \tag{15}$$

$$Sh = \frac{kD_h}{D_a} \tag{16}$$

where D_a is vapor diffusivity in air (m^2/s), D_h is the hydrodynamic diameter (m). For plate-fin channels of finite fin conductance, the fully developed Nusselt and Sherwood numbers are influenced by aspect ratios (a/b), and fin conductance parameters [10]. This is quite different from the simple classical data of a sensible-only heat exchanger with infinite fin conductance [13].

The fin conductance parameter for sensible heat transfer

$$\Omega_s = \frac{\lambda_{fin}\delta_{fin}}{\lambda_a(2a)} \tag{17}$$

where λ_{fin} is heat conductivity of fin, δ_{fin} is fin thickness (m), and $(2a)$ is channel height (m). Fin conductivity is a function of material porosity as

$$\lambda_{fin} = \phi\lambda_{water} + (1-\phi)\lambda_{paper} \tag{18}$$

where ϕ is paper porosity; λ_{water} is heat conductivity of liquid water; λ_{paper} is heat conductivity of dry paper. When the plate material is paper, its heat conductivity is equal to fin. When the plate material is membrane, following should be used

$$\lambda_{pla} = \phi\lambda_{water} + (1-\phi)\lambda_{mem} \tag{19}$$

The fin conductance parameter for moisture transfer

$$\Omega_L = \frac{\rho_{fin}k_p D_{fin}\delta_{fin}}{\rho_a D_a(2a)} \tag{20}$$

where D_{fin} is water diffusivity in fin materials (m^2/s); k_p is partition coefficient which reflects the moisture sorption potential on fin materials. The value of k_p can be measured by adsorption isotherms as

$$\theta = k_p RH \tag{21}$$

where is water uptake in materials (kg moisture/kg material), RH is relative humidity of moist air. The more hydrophilic the materials are, the higher the value of k_p is.

Pressure drop across the channels (Pa) is

$$dP = \frac{x_F}{D_h} 2\rho_a u_a^2 (f_c + f_L) \tag{22}$$

where u_a is mean air velocity in the channels (m/s), f_c is friction coefficient for the channel, f_L is local friction coefficients for the inlet and outlets.

For the sinusoidal cross sectional channel with aspect ratio of 0.4, the product of friction coefficient and Reynolds number is a constant [10,13]

$$f_c \cdot \mathrm{Re} = 11.21 \tag{23}$$

The local friction coefficient can be regressed from experimental measurements, the value for the cores is found to be

$$f_L = 0.009 \tag{24}$$

The Reynolds number

$$\mathrm{Re} = \frac{u_a D_h}{v} \tag{25}$$

where v is hydrodynamic viscosity of air (m^2/s).

3.2. Heat and mass transfer through plates

Heat conduction through the plate is in equilibrium with the convective heat transfer on both sides. Whether it's paper or membrane, the equilibrium can be expressed by

$$(hA)_f(T_f^* - T_{mf}^*) = \frac{A_{pla}\lambda_{pla}}{\delta_{pla}}(T_{mf}^* - T_{me}^*) \tag{26}$$

$$(hA)_e(T_e^* - T_{me}^*) = \frac{A_{pla}\lambda_{pla}}{\delta_{pla}}(T_{mf}^* - T_{me}^*) \tag{27}$$

where A_{pla} is total transfer area (m^2) of plates; λ_{pla} is heat conductivity of plate (kW m^{-1} K^{-1}; δ_{pla} is thickness of plate (m). In above two equations, the right hand sides are heat conduction through plates. They are the same. In the left hand sides, the first equation represents convective heat transfer in fresh air side, and the second equation represents convective heat transfer in exhaust air side.

Moisture diffusion through the plate is in equilibrium with the convective mass transfer on two surfaces. The equations can be expressed by

$$\rho_a(kA)_f(\omega_f - \omega_{mf}) = \frac{\rho_{pla}A_{pla}D_{pla}}{\delta_{pla}}(\theta_{mf} - \theta_{me}) \tag{28}$$

$$\rho_a(kA)_e(\omega_e - \omega_{me}) = \frac{\rho_{pla}A_{pla}D_{pla}}{\delta_{pla}}(\theta_{mf} - \theta_{me}) \tag{29}$$

where D_{pla} is water diffusivity in plate material (m^2/s).

The relation between humidity ratio and RH is [11,12]

$$RH = \frac{\exp(5294/T)}{10^6}\omega \tag{30}$$

Moisture emission rate through the plate from the fresh air to the exhaust air

$$E = \frac{\rho_{pla}D_{pla}}{\delta_{pla}}(\theta_{mf} - \theta_{me}) \tag{31}$$

Combining Eqs. (21), (30) and (31), it is deduced that

$$E = \frac{\rho_{pla} D_{pla} k_p \exp(5294/T)}{10^6 \delta_{pla}} (\omega_{mf} - \omega_{me}) \quad (32)$$

The total number of transfer units for sensible heat transfer and moisture transfer are

$$NTU_{s,tot} = \frac{(UA)_{tot}}{(Gc_p)_f} = \frac{(UA)_{tot}}{(Gc_p)_e} \quad (33)$$

$$NTU_{L,tot} = \frac{(kA)_{tot}}{(Gc_p)_f} = \frac{(kA)_{tot}}{(Gc_p)_e} \quad (34)$$

respectively, where

$$(UA)_{tot}^{-1} = (UA)_f^{-1} + (\frac{A_{pla}\lambda_{pla}}{\delta_{pla}})^{-1} + (UA)_e^{-1} \quad (35)$$

$$(kA)_{tot}^{-1} = (kA)_f^{-1} + \left(\frac{\rho_{pla} A_{pla} D_{pla}}{\rho_a \delta_{pla}}\right)^{-1} + (kA)_e^{-1} \quad (36)$$

In fact, the final sensible effectiveness and the latent effectiveness can be estimated from the total number of transfer units with established correlations [3]. However, to know the details of heat and moisture transfer in the exchanger, detailed equations should be solved.

In Eqs. (33)–(36), a balanced flow, i.e., an equal mass flow rates between fresh side and exhaust air side, are assumed. The assumption is reasonable in most real applications. Though in some cases, unbalanced flow is implemented to have positive or negative pressure indoor ventilation. However, the mass flow unbalance is small. When the mass unbalance is great, different fresh air and exhaust air mass flow rates should be considered.

3.3. Boundary conditions

Fresh:

$$T_f^*|_{x^*=0} = 1 \quad (37)$$

$$\omega_f^*|_{x^*=0} = 1 \quad (38)$$

Exhaust:

$$T_e^*|_{y^*=0} = 0 \quad (38)$$

$$\omega_e^*|_{y^*=0} = 0 \quad (39)$$

3.4. Physical properties

The structural and basic physical parameters of the two cores are listed in Table 1. Based on these parameters, the key transport properties of the two cores are shown in Table 2. As seen, the fin efficiencies are only 50% for heat transfer, and 34% for moisture transfer. The reasons are due to the slow heat conductivity and moisture diffusivity in paper-fin materials [10].

Table 2
Transport properties of the two cores.

Properties	Value
a/b	0.4
Ω_s	0.93
Ω_L	2.8e−5
Nu	1.18
Sh	0.705
$f_c \cdot Re$	11.21
f_L	0.009
k_p	0.58
D_h	1.66
A_f, A_e (m^2)	18.02
A_{pla} (m^2)	7.87
ϕ	0.65

4. Results and discussion

4.1. Solution procedure

A finite difference technique is used to discrete the partial differential equations developed for the air streams. The calculating domain is divided into a number of discrete nodes. Each node represents a control volume. The number of calculating node is 50 in x direction. An upstream differencing scheme is used for two air streams. The two air streams and the asymmetric membrane are closely coupled. Heat transfer and mass transfer are also related to each other. Therefore iterative techniques are needed to solve these equations. A description of the iterative procedure is as following:

(a) Assume initial temperature and humidity fields in the two streams.
(b) Calculate the temperature and humidity values on membrane surfaces by Eqs. (26)–(29).
(c) Taking the current values of temperature and humidity on membrane surfaces as the default values, get the temperature and humidity profiles in two air streams by solving Eqs. (3)–(6).
(d) Go to (c), until the old values and the newly calculated values of temperature and humidity at all calculating nodes are converged.

After these procedures, all the governing equations are solved simultaneously. To assure the accuracy of the results presented, numerical tests were performed for the duct to determine the effects of the grid size. It indicates that 50 grids are adequate (less than 0.1% difference compared with 80 grids). The final numerical uncertainty is 0.1%.

When the temperature and humidity fields in the exchanger are calculated, the sensible and latent effectiveness are calculated using mean outlet values. These are numerically obtained data.

4.2. Experimental validation

The sensible effectiveness of the two cores under various volumetric air flow rates are plotted in Fig. 5. The measured data are demonstrated by discrete dots. The error bars are plotted for the measured values. The calculated data are plotted by a solid line.

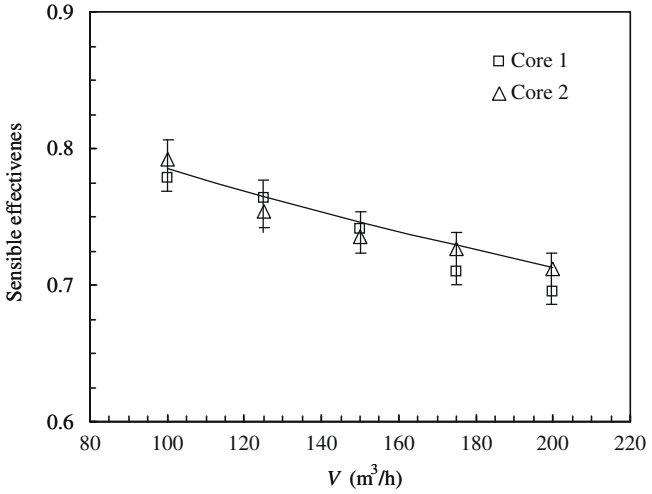

Fig. 5. Sensible effectiveness of the two plate-fin heat mass exchangers under various air flow rates. The solid line is the calculated values, and the discrete dots are the measured data.

The calculated sensible effectiveness is the same for the two cores. The reason is that in the core, the heat transfer resistance is mainly in air sides, and the resistance in plates is negligible. The two cores have the same air side resistance, which determines the sensible effectiveness. The different resistance in plate has little influence on sensible hat transfer. The maximum deviation between the calculated value and the measured data is below 5%, indicating the performance is predicted satisfactorily. The sensible effectiveness is rather high. As seen, the sensible effectiveness is from 0.78 to 0.7, showing sufficient heat transfer between the fresh air and the exhaust air, even with the fins of low fin conductance parameter as paper. In other words, the current paper-fin and paper-plate core already has high performance for sensible heat recovery. Replacing it with a paper-fin membrane-plate core will have little use in further increasing its performance in sensible heat recovery.

The latent effectiveness of the two cores under various volumetric air flow rates are plotted in Fig. 6. As before, the measured data are demonstrated by discrete dots with error bars. The calculated data are plotted by two solid lines. Contrary to sensible effectiveness, the calculated latent effectiveness is quite different from each other for the two cores. The first core has a low latent effectiveness. However, the core 2 of paper-fin and membrane-plate has a 60% higher latent effectiveness than the core 1 of paper-fin and paper-plate. The reason is that in the core, the moisture transfer resistance is mainly in plate side, and the resistance in air side is the same for the two cores. The moisture diffusivity in membrane is 15 times higher than that in paper. The result is that core 2 has higher moisture recovery effectiveness than core 1. The latent effectiveness of the current paper-fin paper-plate core is only unsatisfactorily from 0.3 to 0.4. However, the new core of paper-fin and membrane-plate has an ideal performance of latent effectiveness from 0.6 to 0.7. Great improvements have been made with the new design. Further, the model predicts the latent effectiveness quite well. A maximum deviation is only 5.5%.

The pressure drops of the two cores are plotted in Fig. 7. The two cores have the same numerical values of pressure drop (the line). This is due to the same structures and geometries. However, experimental results found the new core of paper-fin and membrane-plate has a relatively higher pressure drop than the old core of paper-fin and paper-plate. The reason may be that the membranes made are more coarse than paper and they have a greater resistance to flow. Generally, from these three figures, it can be concluded that the new core has a 60% higher latent effectiveness than the old core. The model developed is valid and is satisfactory in predicting performance.

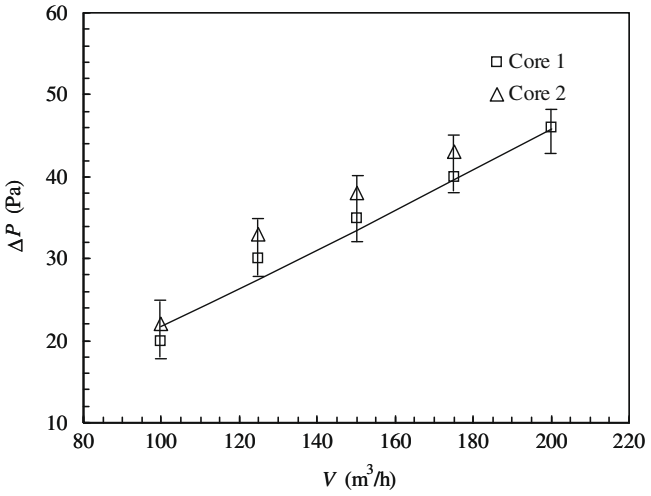

Fig. 7. Pressure drop of the two plate-fin heat mass exchangers under various air flow rates. The solid lines are the calculated values, and the discrete dots are the measured data.

4.3. Heat mass transfer in air streams

The model can disclose details inside the channel that the experiment cannot. Temperature and humidity fields in the air streams are calculated for the nominal operating conditions. The dimensionless temperature fields are shown in Fig. 8 for the fresh air and in Fig. 9 for the exhaust air, respectively. The dimensionless temperature of the plate is shown in Fig. 10. The core is paper-fin and membrane-plate.

As seen from these figures, the temperature of fresh air decreases along the flow in x direction, while the temperature of the exhaust increases along the flow in y direction. Because the two flows are in cross-flow arrangement, the temperature profiles exhibit a two-dimensional nature. The plate temperature is almost equal to the average temperature of the fresh air and exhaust air, meaning little conductance resistance in plate.

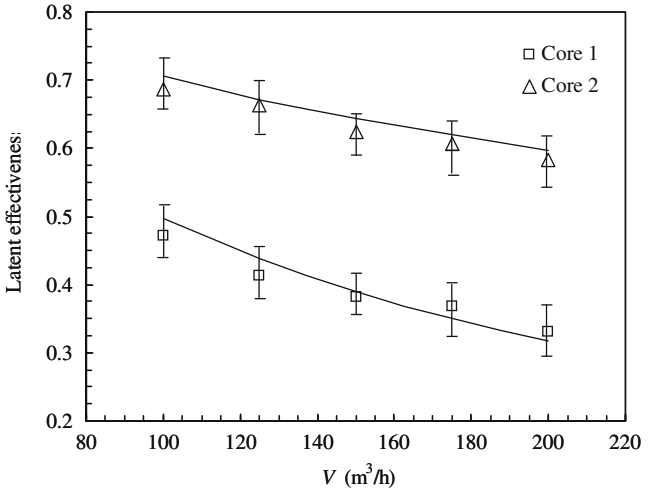

Fig. 6. Latent effectiveness of the two plate-fin heat mass exchangers under various air flow rates. The solid lines are the calculated values, and the discrete dots are the measured data.

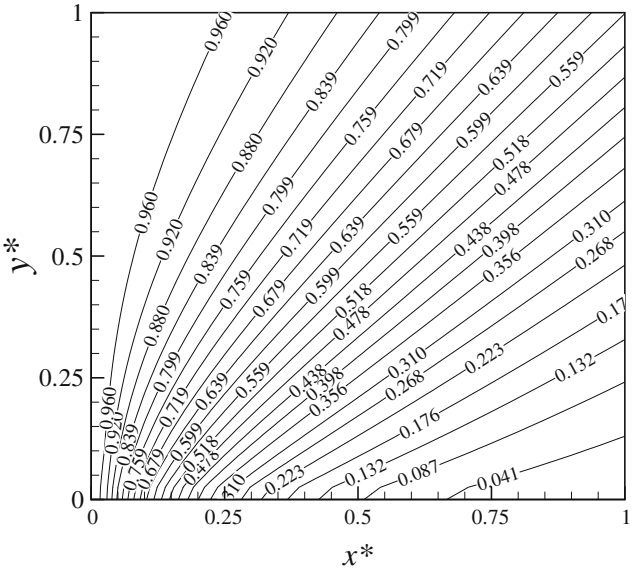

Fig. 8. Dimensionless temperature of fresh air.

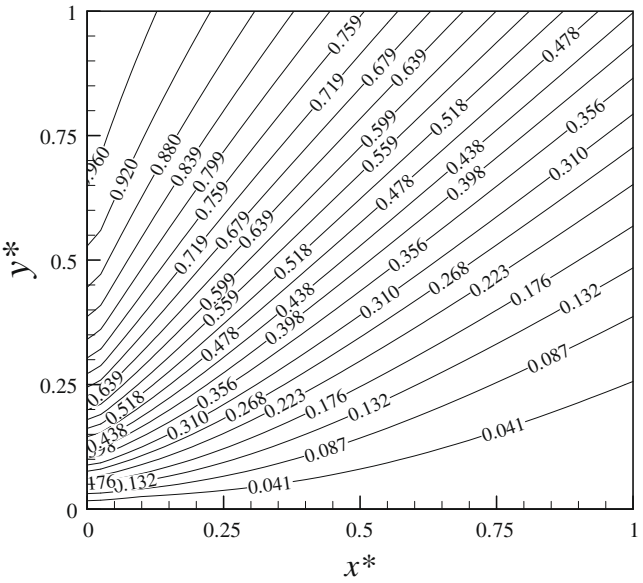

Fig. 9. Dimensionless temperature of exhaust air.

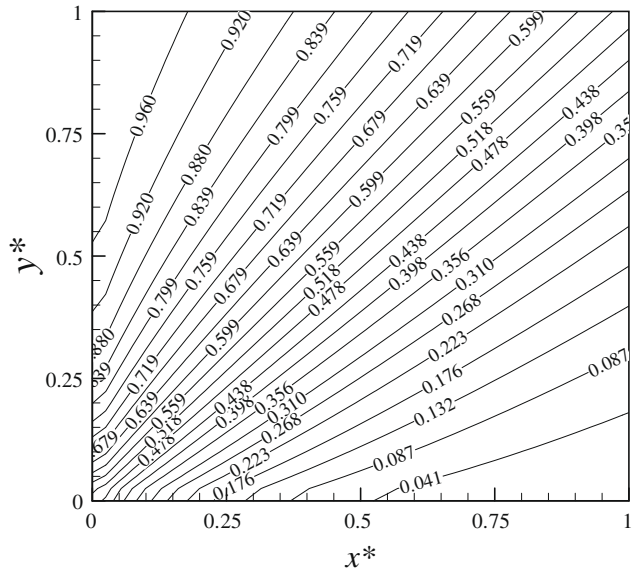

Fig. 10. Dimensionless temperature of membrane temperature.

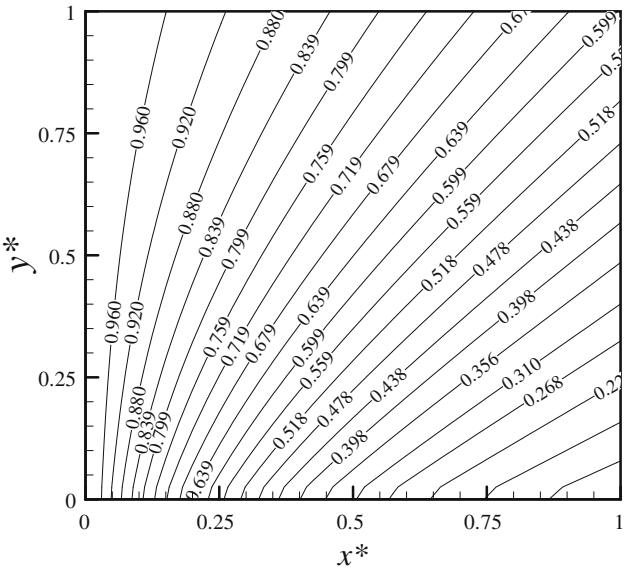

Fig. 11. Dimensionless humidity of fresh air.

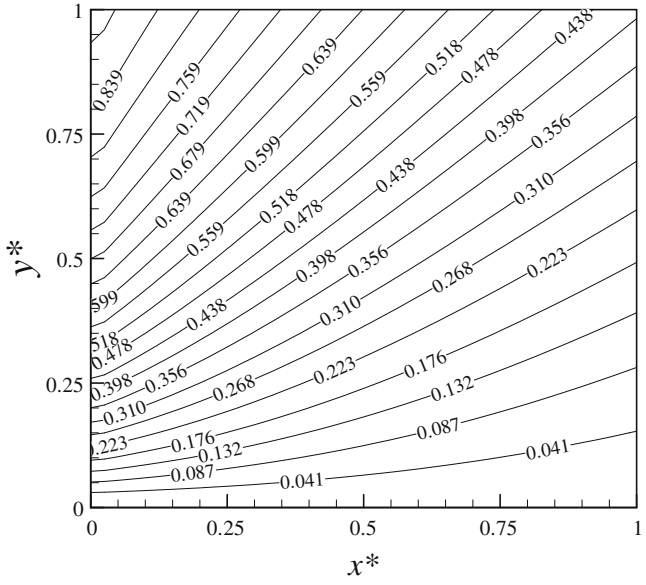

Fig. 12. Dimensionless humidity of exhaust air.

The dimensionless humidity profiles are shown in Fig. 11 for the fresh air stream and in Fig. 12 for the exhaust air stream for core 2. The trends are similar to temperature profiles. However, the mass transfer resistance for plate, even it's membrane, is larger than heat transfer resistance, so the humidity changes more slowly than humidity does. In summary, moisture resistance in plate is the dominant resistance in the core.

The humidity on membrane surface in fresh air side is shown in Fig. 13 and the humidity on membrane surface in exhaust air surface is shown in Fig. 14, respectively. As seen, the two surfaces have distinct humidity differences on two surfaces, showing the dominant effect of moisture diffusion resistance in plate. Therefore, to intensify moisture transfer in enthalpy exchangers, it is necessary to use plate materials that have high moisture diffusivities.

The local moisture permeation rates through the membrane are shown in Fig. 15 for the paper core and Fig. 16 for the membrane core. In both cases, the highest moisture emission rates are located on the surfaces where the two air streams interconnect, since here the driving force is the highest. It is also observed that the emission rates through the membrane-plate are far higher than those through the paper-plate. This is just the reason that the core 2 has 60% higher latent effectiveness than core 1.

5. Conclusions

To solve the problem of low latent effectiveness with common all-paper cores, a novel composite supported liquid membrane is used as the new material for the plate, while still keeping the paper as the fin materials. A detailed experiment is done to study the exchanger performance. In combination with mathematical modeling, following results can be found:

(1) The new membrane core has an equal sensible effectiveness with the old all-paper core. However, the latent effectiveness is 60% higher than the old one. The two cores have the same pressure drops.

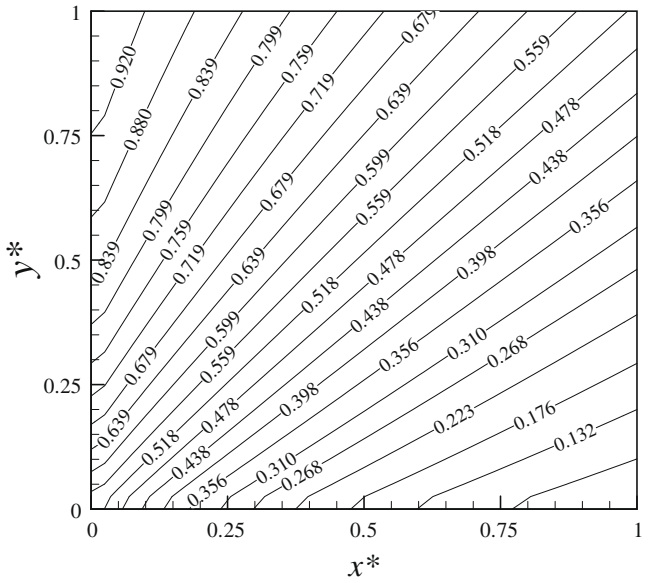

Fig. 13. Dimensionless humidity of membrane surface on fresh air side.

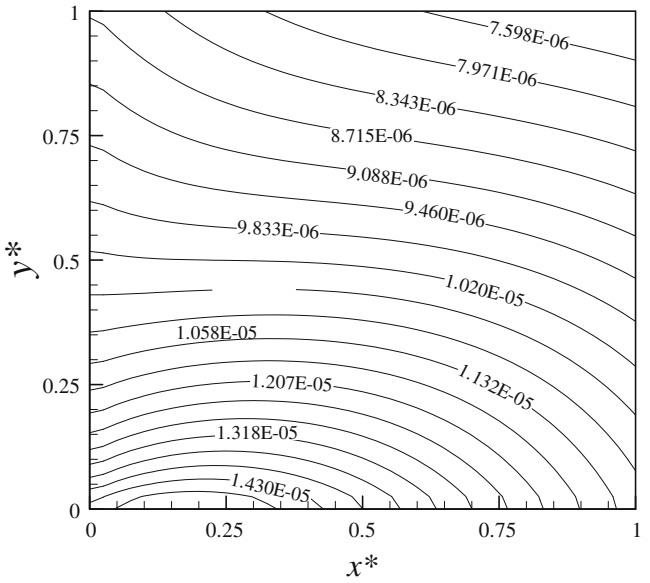

Fig. 15. Emission rate on plate surface for core 1 of paper-plate (kg m^{-2} s^{-1}).

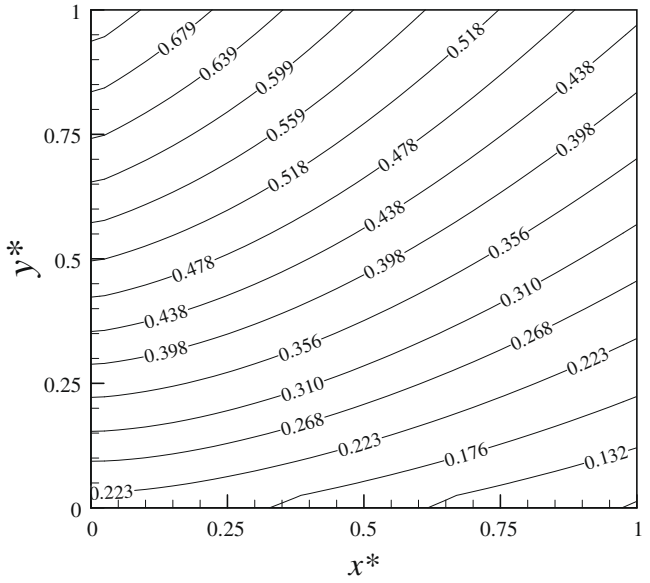

Fig. 14. Dimensionless humidity of membrane surface on exhaust air side (kg m^{-2} s^{-1}).

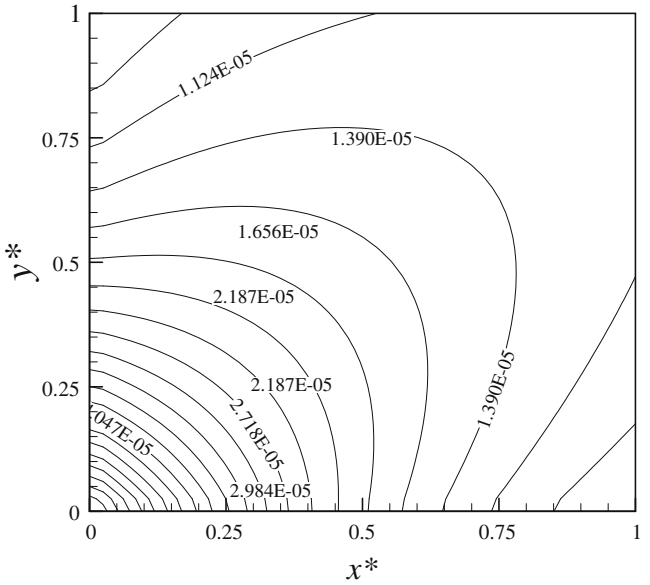

Fig. 16. Emission rate on plate surface for core 2 of membrane-plate.

(2) The main resistance for heat transfer is in air side, so to enhance heat transfer with fins is useful. However, the major resistance for mass transfer is in plate itself, so fins will have little use. Rather, using high vapor permeable materials like composite supported liquid membrane as the plates is the only solution. The emission rates through the membrane-plate are far higher than those through the paper-plate. The paper-fin and membrane-plate core have high sensible effectiveness and latent effectiveness at the same time.

(3) The semi-lumped parameter model can predict the exchanger performance very well. It can be used to optimize enthalpy exchangers in future. The transport mechanisms inside the channel can be disclosed with the mathematical modeling.

Acknowledgements

This Project 50676034 is supported by National Natural Science Foundation of China. The project is also supported by the National High Technology Research and Development Program of China (863), 2008AA05Z206; and National Key Project of Scientific and Technical Supporting Programs, No. 2006BAA04B02.

References

[1] L.G. Harriman, J. Judge, Dehumidification equipment advances, ASHRAE J. 44 (8) (2002) 22–29.
[2] K.R. Kistler, E.L. Cussler, Membrane modules for building ventilation, Chem. Eng. Res. Des. 80 (2002) 53–64.
[3] L.Z. Zhang, J.L. Niu, Effectiveness correlations for heat and moisture transfer processes in an enthalpy exchanger with membrane cores, ASME J. Heat Transfer 124 (5) (2002) 922–929.

[4] C.Y. Pan, C.D. Jensen, C. Bielech, H.W. Habgood, Permeation of water vapor through cellulose triacetate membranes in hollow fiber form, J. Appl. Poly. Sci. 22 (1978) 2307–2323.
[5] F. Debeaufort, A. Voilley, P. Meares, Water vapor permeability and diffusivity through methylcellulose edible films, J. Membrane Sci. 91 (1994) 125–133.
[6] E.L. Cussler, Diffusion-Mass Transfer in Fluid systems, Cambridge University Press, 2000.
[7] C. Isetti, E. Nannei, A. Magrini, On the application of a membrane air–liquid contactor for air dehumidification, Energ. Buildings 15 (1997) 185–193.
[8] L.Z. Zhang, Fabrication of a Lithium Chloride solution based composite supported liquid membrane and its moisture permeation analysis, J. Membrane Sci. 276 (1–2) (2006) 91–100.
[9] L.Z. Zhang, F. Xiao, Simultaneous heat and moisture transfer through a composite supported liquid membrane, Int. J. Heat Mass Transfer 51 (9–10) (2008) 2179–2189.
[10] L.Z. Zhang, Heat and mass transfer in plate-fin sinusoidal passages with vapor-permeable wall materials, Int. J. Heat Mass Transfer 51 (3–4) (2008) 618–629.
[11] J.L. Niu, L.Z. Zhang, Membrane-based enthalpy exchanger: material considerations and clarification of moisture resistance, J. Membrane Sci. 189 (2001) 179–191.
[12] C.J. Simonson, R.W. Besant, Energy wheel effectiveness: part I – development of dimensionless groups, Int. J. Heat Mass Transfer 42 (1999) 2161–2170.
[13] R.K. Shah, A.L. London, Laminar Flow Forced Convection in Ducts, Academic Press, Inc., New York, 1978.